

Search for New Physics in Lepton + Photon + X Events with 929 pb^{-1} of $p\bar{p}$ Collisions at $\sqrt{s}= 1.96 \text{ TeV}$

A.Loginov *

ITEP, Moscow

June 12, 2021

Abstract

We present results of a search in $929 \pm 56 \text{ pb}^{-1}$ of $p\bar{p}$ collisions at 1.96 TeV for the anomalous production of events containing a charged lepton (ℓ , either e or μ) and a photon (γ), both with high transverse momentum, accompanied by additional signatures, X, including missing transverse energy (\cancel{E}_T) and additional leptons and photons. We use the same selection criteria as in the previous CDF Run I search, but with an order-magnitude larger data set, a higher $p\bar{p}$ collision energy, and the CDF II detector.

1 Introduction

The signature of high- E_T [1] leptons and photons ($\ell\gamma+X$) appears in a variety of physics beyond the Standard Model (SM) [2], so called New Physics (NP) scenarios, such as Technicolor, Gauge-Mediated Supersymmetry, LED.

While it is good to be guided by theory, one should also remain open to the unexpected. Therefore we use the technique of a Signature-Based Search, and look for significant deviations from the SM [3, 4] in $\ell\gamma+X$ events, which include the production of fundamental particles, such as γ , Z^0 , W^\pm .

In Run I, in a sample of 86 pb^{-1} of $p\bar{p}$ collisions at an energy of 1.80 TeV, the CDF experiment observed a single clean event consistent with having a pair of high- E_T electrons, two high- E_T photons, and large \cancel{E}_T [3]. A subsequent search for ‘cousins’ of the $ee\gamma\gamma\cancel{E}_T$ signature in the inclusive signature $\ell\gamma+X$ found 16 events with a SM expectation of 7.6 ± 0.7 events, corresponding in likelihood to a 2.7σ effect [4].

*For the CDF Collaboration

In this proceedings we report the preliminary results of extending the Run II $\ell\gamma+X$ search [5] to the full data set taken during the period March 2002 through February, 2006, an exposure of $929 \pm 56 \text{ pb}^{-1}$. We also present the details of the results for the $e\mu\gamma + X$ signature.

2 The CDF II Detector

The CDF II detector is a cylindrically symmetric spectrometer designed to study $p\bar{p}$ collisions at the Fermilab Tevatron based on the same solenoidal magnet and central calorimeters as the CDF I detector [6] from which it was upgraded. Because the analysis described here is intended to repeat the Run I search as closely as possible, we note especially the differences from the CDF I detector relevant to the detection of leptons, photons, and \cancel{E}_T . The tracking systems used to measure the momenta of charged particles have been replaced with a central outer tracker (COT) with smaller drift cells [7], and an enhanced system of silicon strip detectors [8]. The calorimeters in the regions [9] with pseudorapidity $|\eta| > 1$ have been replaced with a more compact scintillator-based design, retaining the projective geometry [10]. The coverage in φ of the CMP and CMX muon systems [11] has been extended; the CMU system is unchanged.

3 Selection of $\ell\gamma+X$ Events

The identification of leptons and photons is essentially the same as in the Run I search [4], with only minor technical changes. The identification criteria for the results for the full dataset presented here are identical to those used for the first third, presented in Refs [5].

Inclusive $\ell\gamma$ events are selected by requiring a central ($|\eta| \lesssim 1.0$) γ candidate with $E_T^\gamma > 25 \text{ GeV}$ and a central e or μ with $E_T^\ell > 25 \text{ GeV}$.

Additional leptons in the central region are required to have $E_T^\ell > 20 \text{ GeV}$, and electrons in endplug calorimeters should have $E_T^e > 15 \text{ GeV}$.

Missing transverse energy \cancel{E}_T is calculated from the calorimeter tower energies in the region $|\eta| < 3.6$. Corrections are then made to the \cancel{E}_T for non-uniform calorimeter response [12] for jets with uncorrected $E_T > 15 \text{ GeV}$ and $|\eta| < 2.0$, and for muons with $p_T > 20 \text{ GeV}$.

The variable H_T is defined for each event as the sum of the transverse energies of the leptons, photons, jets, and \cancel{E}_T .

Because we are looking for processes with small cross sections, and hence

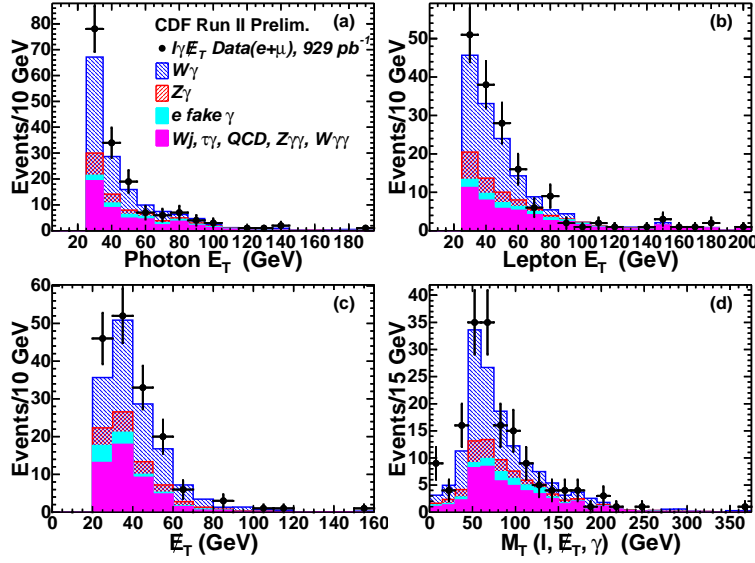


Figure 1: The distributions for events in the $l\gamma\cancel{E}_T$ sample (points) in a) the E_T of the photon; b) the E_T of the lepton (e or μ); c) the missing transverse energy, \cancel{E}_T ; and d) the transverse mass of the $l\gamma\cancel{E}_T$ system. The histograms show the expected SM contributions, including estimated backgrounds from misidentified photons and leptons.

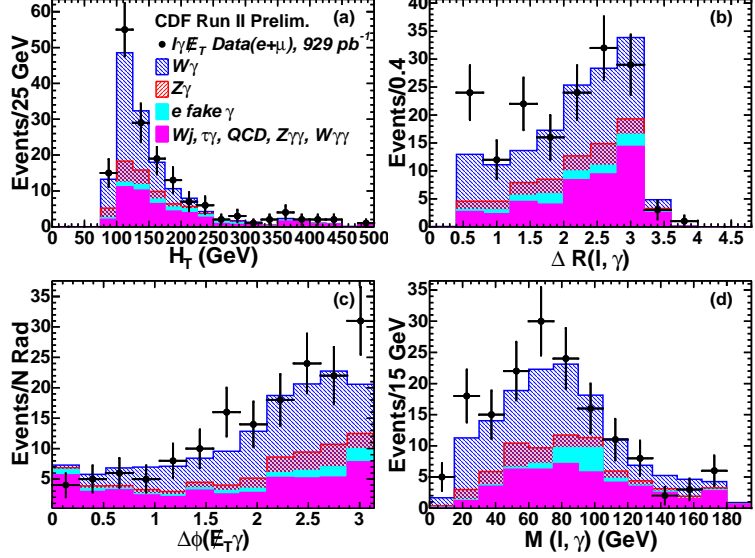


Figure 2: The distributions for events in the $l\gamma\cancel{E}_T$ sample (points) in a) H_T , the sum of the transverse energies of the lepton, photon, jets and \cancel{E}_T ; b) the distance in η - ϕ space between the photon and lepton; c) the angular separation in ϕ between the lepton and the missing transverse energy, \cancel{E}_T ; and d) the invariant mass of the $l\gamma$ system. The histograms show the expected SM contributions, including estimated backgrounds from misidentified photons and leptons.

small numbers of measured events, we use larger control samples to validate our understanding of the detector performance and to measure efficiencies and backgrounds.

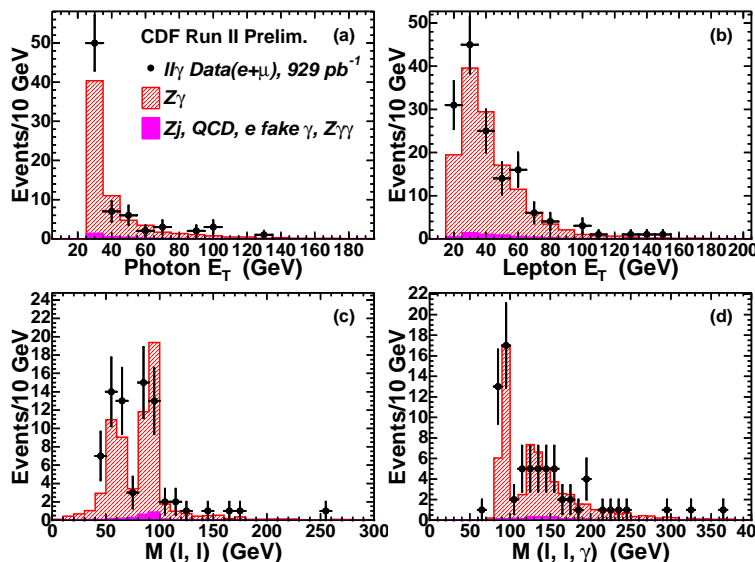


Figure 3: The distributions for events in the $l\ell\gamma$ sample (points) in a) the E_T of the photon; b) the E_T of the leptons (two entries per event); c) the 2-body mass of the dilepton system; and d) the 3-body mass $m_{l\ell\gamma}$. The histograms show the expected SM contributions.

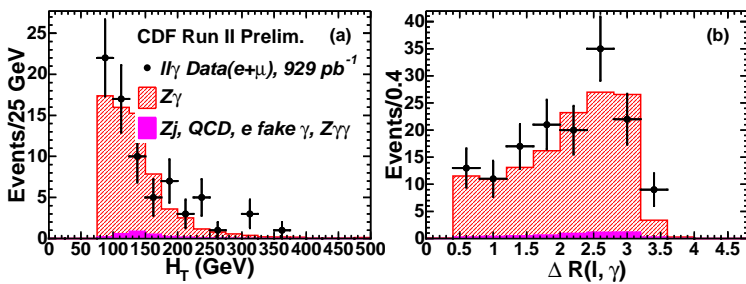


Figure 4: The distributions for events in the $l\ell\gamma$ sample (points) in a) H_T , the sum of the transverse energies of the lepton, photon, jets and \cancel{E}_T ; b) the distance in η - ϕ space between the photon and each of the two leptons. The histograms show the expected SM contributions, including estimated backgrounds from misidentified photons and leptons.

We use W^\pm and Z^0 production derived from the same inclusive lepton datasets as control samples to ensure that the efficiencies for high- p_T electrons and muons are well understood. In addition, the W^\pm samples provide the control samples for the understanding of \cancel{E}_T . The photon control sample is constructed from $Z^0 \rightarrow e^+e^-$ events in which one of the electrons radiates a high- E_T γ such that the $e\gamma$ invariant mass is within 10 GeV of the Z^0 mass.

The first search we perform is in the $l\gamma\cancel{E}_T + X$ subsample, defined by requiring that an event contain $\cancel{E}_T > 25$ GeV in addition to the γ and “tight” lepton.

The electron and muon kinematic distributions are combined in Figures 1 and 2. There is very good agreement with the expected SM shapes [13].

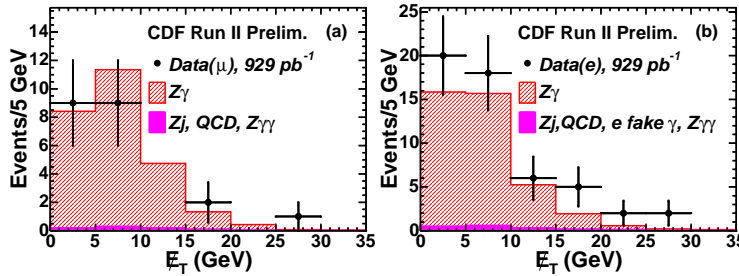


Figure 5: The distributions in missing transverse energy \cancel{E}_T observed in the inclusive search for a) $\mu\mu\gamma$ events and b) $ee\gamma$ events. The histograms show the expected SM contributions.

A second search, for the $ll\gamma + X$ signature, is constructed by requiring another e or μ in addition to the “tight” lepton and the γ . The combined distributions for electrons and muons are shown in Figures 3 and 4 [13].

We do not expect SM events with large \cancel{E}_T in the $ll\gamma$ sample; the Run I $ee\gamma\cancel{E}_T$ event was of special interest in the context of supersymmetry [14] due to the large value of \cancel{E}_T (55 ± 7 GeV). Figure 5 shows the distributions in \cancel{E}_T for the $\mu\mu\gamma$ and $ee\gamma$ subsamples of the $ll\gamma$ sample. We observe 3 $ll\gamma$ events with $\cancel{E}_T > 25$ GeV.

4 Standard Model Expectations

The dominant SM source of $l\gamma$ events is electroweak W and Z^0/γ^* production along with a γ radiated from one of the charged particles involved in the process [15]. The number of such events is estimated using leading-order (LO) event generators [16, 17, 18]. Initial state radiation is simulated by the PYTHIA shower Monte Carlo (MC) code [19] tuned to reproduce the underlying event. The generated particles are then passed through a full detector simulation, and these events are then reconstructed with the same code used for the data. We have used both MADGRAPH [16] and COMPHEP[18] to simulate the triboson channels $W\gamma\gamma$ and $Z\gamma\gamma$. A correction for higher-order processes (K-factor) that depends on both the dilepton mass and photon E_T has been applied [20]. to $W\gamma$, $Z^0\gamma$, $W\gamma\gamma$ and $Z^0\gamma\gamma$.

High p_T photons are copiously created from hadron decays in jets initiated by a scattered quark or gluon. In particular, mesons such as the π^0 or η decay to photons which may satisfy the photon selection criteria. The numbers of $lj+X$, $j \rightarrow \gamma$ events expected in the $l\gamma\cancel{E}_T$ and $ll\gamma$ samples are determined by measuring energy in the calorimeter nearby the photon candidate.

The numbers of $lj+X$, $j \rightarrow \gamma$ events expected in the $l\gamma\gamma$ and $e\mu\gamma$ samples are determined by measuring the jet E_T spectrum in $l\gamma+\text{jet}$, $l+\text{jets}$ and

Table 1: A comparison of the numbers of events predicted by the SM and the observations for the $\ell\gamma\cancel{E}_T$ signature. The SM predictions are dominated by $W\gamma$ and $Z^0\gamma$ production [16, 17, 18]. Other contributions come from $W\gamma\gamma$ and $Z^0\gamma\gamma$, leptonic τ decays, and misidentified leptons, photons, or \cancel{E}_T .

CDF Run II Preliminary, 929pb ⁻¹			
Lepton+ Gamma + \cancel{E}_T Events			
Standard Model Source	$e\gamma\cancel{E}_T$	$\mu\gamma\cancel{E}_T$	$(e + \mu)\gamma\cancel{E}_T$
$W^\pm\gamma$	41.65 ± 4.84	29.85 ± 5.62	71.50 ± 10.01
$Z^0/\gamma + \gamma$	3.65 ± 1.31	14.10 ± 2.36	17.75 ± 3.65
$W^\pm\gamma\gamma$	0.32 ± 0.042	0.18 ± 0.025	0.50 ± 0.064
$Z^0/\gamma + \gamma\gamma$	0.087 ± 0.012	0.38 ± 0.048	0.47 ± 0.058
$t\bar{t}\gamma$	0.22 ± 0.029	0.13 ± 0.019	0.35 ± 0.045
$Z^0 \rightarrow e^+e^-, e \rightarrow \gamma$	9.59 ± 0.76	–	9.59 ± 0.76
Jet faking γ	21.5 ± 4.8	6.2 ± 3.6	27.7 ± 6.0
$\tau\gamma$ contribution	2.15 ± 0.56	0.76 ± 0.24	2.91 ± 0.65
QCD(Jets faking ℓ and \cancel{E}_T)	15.0 ± 4.12	0.0 ± 0.1	15.0 ± 4.12
DIF (Decays-In-Flight)	–	2.3 ± 0.72	2.3 ± 0.72
Total	$94.17 \pm 8.14(tot)$	$53.90 \pm 7.11(tot)$	$148.07 \pm 12.97(tot)$
Observed in Data	96	67	163

$e\mu$ +jet samples, respectively, and then multiplying by the probability of a jet being misidentified as a photon, $P_\gamma^{jet}(E_T)$, which is measured in data samples triggered on jets [15].

To estimate the numbers of $\ell e+X$, $e \rightarrow \gamma$ expected events we measure P_γ^e , the probability that an electron undergoes hard bremsstrahlung and is misidentified as a photon. P_γ^e is measured from the photon control sample. We then apply this misidentification rate to electrons in the $\ell e+X$ samples.

We have estimated the background due to events with jets misidentified as $\ell\gamma\cancel{E}_T$ or $\ell\ell\gamma$ signatures by studying the total p_T of tracks in a cone in $\eta - \varphi$ space of radius $R = 0.4$ around the lepton track [21].

There is a muon background that we expect escapes the above method: a low-momentum hadron, not in an energetic jet, decays to a muon in a configuration that a high-momentum track is reconstructed from the initial track segment due to the hadron and the secondary track segment from the muon [22]. The contribution from this background is estimated by identifying tracks consistent with a “kink” in the COT.

5 Results

The predicted and observed totals for the $\ell\gamma\cancel{E}_T$ and $\ell\ell\gamma$ searches are shown in Tables 1 and 2, respectively. We observe 163 $\ell\gamma\cancel{E}_T$ events, versus the

Table 2: A comparison of the numbers of events predicted by the SM and the observations for the $\ell\gamma\cancel{E}_T$ signature. The SM predictions are dominated by $Z^0\gamma$ production [16, 17, 18]. Other contributions come from $Z^0\gamma\gamma$, and misidentified leptons, photons, or \cancel{E}_T .

CDF Run II Preliminary, 929pb⁻¹			
Multi-Lepton + Photon Predicted Events			
SM Source	$ee\gamma$	$\mu\mu\gamma$	$ll\gamma$
$Z^0\gamma$	37.85 ± 4.65	25.55 ± 2.88	63.40 ± 7.48
$Z^0\gamma\gamma$	0.72 ± 0.088	0.40 ± 0.050	1.12 ± 0.13
Z^0 +Jet, jet faking γ	0.0 ± 1.20	0.0 ± 1.10	0.0 ± 1.60
$Z^0 \rightarrow e^+e^-, e \rightarrow \gamma$	0.38 ± 0.11	–	0.38 ± 0.11
QCD (Non-WZ) fakes	0.0 ± 0.20	0.0 ± 0.1	0.0 ± 0.20
DIF (Decays-In-Flight)	–	0.0 ± 0.20	0.0 ± 0.20
Total	$38.95 \pm 4.8(tot)$	$25.95 \pm 3.09(tot)$	$64.93 \pm 7.65(tot)$
Observed	53	21	74

Table 3: A comparison of the numbers of events predicted by the SM and the observations for the $e\mu\gamma$ signature. The SM predictions are dominated by $Z^0\gamma$ production [16, 17, 18]. Other contributions come from $W\gamma$, $Z^0\gamma\gamma$, $W\gamma\gamma$, and misidentified leptons, photons, or \cancel{E}_T .

CDF Run II Preliminary, 929pb⁻¹	
$e\mu + \text{Photon} + X$ Events	
Standard Model Source	$e\mu\gamma + X$
$Z^0\gamma$	0.66 ± 0.088
$W\gamma$	0.095 ± 0.18
$Z^0\gamma\gamma$	0.057 ± 0.0054
$W\gamma\gamma$	0.011 ± 0.0028
$e\mu j, j \rightarrow \gamma$	0.05 ± 0.007
$ee\mu, e \rightarrow \gamma$	0.063 ± 0.045
$\tau\gamma$ contribution	0.089 ± 0.18
Total	1.01 ± 0.33
Observed	0

expectation of 148.07 ± 12.97 events. The predicted and observed kinematic distributions for the $\ell\gamma\cancel{E}_T$ signature (the sum of electrons and muons) are compared in Figures 1 and 2 [13].

In the $ll\gamma$ channel, we observe 74 events, versus an expectation of 64.93 ± 7.65 events. There is no significant excess in either signature. The predicted and observed kinematic distributions for the $ll\gamma$ signature are compared in Figures 3, 4 and 5 [13].

The predicted and observed totals for the $\ell\gamma\gamma$ and $e\mu\gamma$ searches are shown in Tables 3 and 4, respectively. We observe no $\ell\gamma\gamma$ or $e\mu\gamma$ events, versus the expectation of 0.62 ± 0.15 and 1.01 ± 0.33 events, respectively.

Table 4: A comparison of the numbers of events predicted by the SM and the observations for the $\ell\gamma\gamma$ signature. The SM predictions are dominated by $Z^0\gamma\gamma$ production [16, 18]. Dominant contribution comes from misidentified photons.

CDF Run II Preliminary, 929pb ⁻¹			
Multi-Photon + Lepton Events			
SM Source	$e\gamma\gamma$	$\mu\gamma\gamma$	$\ell\gamma\gamma$
$W^\pm\gamma\gamma$	0.021 ± 0.0043	0.015 ± 0.0034	0.036 ± 0.0055
$Z^0\gamma\gamma$	0.045 ± 0.005	0.038 ± 0.005	0.083 ± 0.007
$Z^0\gamma, e \rightarrow \gamma$	0.413 ± 0.116	-	0.413 ± 0.116
$\ell jj, \ell\gamma j, j \rightarrow \gamma$	0.05 ± 0.05	0.05 ± 0.05	0.10 ± 0.10
Total	0.53 ± 0.13	0.10 ± 0.05	0.62 ± 0.15
Observed	0	0	0

6 Conclusions

To test whether something new was really there in either the $\ell\ell\gamma\cancel{E}_T$ or $\ell\gamma\cancel{E}_T$ signatures in Run I, we have repeated the $\ell\gamma+X$ search with the same kinematic requirements as the Run I search, but with an exposure more than 10 times larger, $929 \pm 56 \text{ pb}^{-1}$, a higher $p\bar{p}$ collision energy, 1.96 TeV, and the CDF II detector [23].

We observe 163 $\ell\gamma\cancel{E}_T$ events, versus an expectation of 148.07 ± 12.97 events from SM physics and background sources. In the $\ell\ell\gamma$ channel, we observe 74 events, versus an expectation of 64.93 ± 7.65 events. There is no significant excess in either signature. We can conclude that the 2.7σ effect observed in Run I, measured with the same criteria and a very similar detector, was a fluctuation.

With respect to the Run I $ee\gamma\gamma\cancel{E}_T$ event, we observe no $\ell\gamma\gamma$ events versus an expectation of 0.62 ± 0.15 events. We do find 3 $\ell\ell\gamma$ events with $\cancel{E}_T > 25$ GeV, versus an expectation of 0.6 ± 0.1 events, corresponding to a likelihood of 2.4 %. We do not consider this significant, and there is nothing in these 3 events to indicate they are due to anything other than a fluctuation. The $ee\gamma\gamma\cancel{E}_T$ event thus remains a single event selected *a posteriori* as interesting, but whether it was from SM $WW\gamma\gamma$ production, a rare background, or a new physics process we cannot determine.

Lastly, we observe no $e\mu\gamma$ events, versus a SM expectation of 1.01 ± 0.33 events.

References

- [1] Transverse momentum and energy are defined as $p_T = p \sin \theta$ and $E_T = E \sin \theta$, respectively. Missing E_T (\vec{E}_T) is defined by $\vec{E}_T = -\sum_i E_T^i \hat{n}_i$, where i is the calorimeter tower number for $|\eta| < 3.6$ (see Ref. [9]), and \hat{n}_i is a unit vector perpendicular to the beam axis and pointing at the i^{th} tower. We correct \vec{E}_T for jets and muons. We define the magnitude $E_T = |\vec{E}_T|$. We use the convention that “momentum” refers to pc and “mass” to mc^2 .
- [2] S.L. Glashow, Nucl. Phys. **22** 588, (1961); S. Weinberg, Phys. Rev. Lett. **19** 1264, (1967); A. Salam, Proc. 8th Nobel Symposium, Stockholm, (1979).
- [3] F. Abe *et al.* (CDF Collaboration), Phys. Rev. D **59**, 092002 (1999); F. Abe *et al.* (CDF Collaboration), Phys. Rev. Lett. **81**, 1791 (1998); D. Toback, Ph.D. thesis, University of Chicago, 1997.
- [4] D. Acosta *et al.* (CDF Collaboration), Phys. Rev. D **66**, 012004 (2002); D. Acosta *et al.* (CDF Collaboration), Phys. Rev. Lett. **89**, 041802 (2002); J. Berryhill, Ph.D. thesis, University of Chicago, 2000.
- [5] A. Abulencia *et al.* (CDF Collaboration), Phys. Rev. Lett. **97**, 031801 (2006); A. Loginov (for the CDF Collaboration), Eur.Phys.J. C **46**, Supplement 2, pp. 21-31 (2006); A. Loginov, Ph.D thesis, Institute for Theoretical and Experimental Physics, Moscow, Russia, September, 2006.
- [6] F. Abe *et al.* (CDF Collaboration), Nucl. Instrum. Methods A **271**, 387 (1988).
- [7] A. Affolder *et al.*, Nucl. Instrum. Methods A **526**, 249 (2004).
- [8] A. Sill *et al.*, Nucl. Instrum. Methods A **447**, 1 (2000); A. Affolder *et al.*, Nucl. Instrum. Methods A **453**, 84 (2000); C.S. Hill, Nucl. Instrum. Methods A **530**, 1 (2000).
- [9] The CDF coordinate system of r , φ , and z is cylindrical, with the z -axis along the proton beam. The pseudorapidity is $\eta = -\ln(\tan(\theta/2))$.
- [10] S. Kuhlmann *et al.*, Nucl. Instrum. Methods A **518**, 39, 2004.
- [11] The CMU system consists of gas proportional chambers in the region $|\eta| < 0.6$; the CMP system consists of chambers after an additional meter of steel, also for $|\eta| < 0.6$. The CMX chambers cover $0.6 < |\eta| < 1.0$.

- [12] A. Bhatti *et al.*, accepted to Nucl. Instrum. Methods, 2006.
- [13] There are no overflows in any of the figures in this paper.
- [14] S. Ambrosanio, G.L. Kane, G.D. Kribs, S.P. Martin, and S. Mrenna, Phys. Rev. D **55**, 1372 (1997); B.C. Allanach, S. Lola, K. Sridhar, Phys. Rev. Lett. **89**, 011801 (2002).
- [15] D. Acosta *et al.* (CDF Collaboration), Phys. Rev. Lett. **94**, 041803 (2005).
- [16] T. Stelzer and W. F. Long, Comput. Phys. Commun. **81**, 357 (1994); F. Maltoni and T. Stelzer, JHEP **302**, 27 (2003).
- [17] U. Baur, T. Han, and J. Ohnemus, Phys. Rev. D **48**, 5140 (1993); J. Ohnemus, Phys. Rev. D **47**, 940 (1993).
- [18] E. Boos *et al.* (The COMPHEP Collaboration), Nucl. Instrum. Methods A **534**, 250, (2004).
- [19] T. Sjostrand, Comput. Phys. Commun. **82** (1994) 74; S. Mrenna, Comput. Phys. Commun. **101** (1997) 232.
- [20] U. Baur, T. Han and J. Ohnemus, Phys. Rev. D **48**, 5140 (1993); U. Baur, T. Han and J. Ohnemus, Phys. Rev. D **57**, 2823 (1998). Both the $W\gamma$ and $Z\gamma$ K-factors are fixed at 1.36 for generated $\ell\nu$ masses below 76 GeV and for generated $\ell^+\ell^-$ masses below 86 GeV. Above the poles the K-factors grow with E_T^γ to be 1.62 and 1.53 at $E_T^\gamma = 100$ GeV for $W\gamma$ and $Z\gamma$, respectively.
- [21] In each signature the background distribution is derived from the observed distribution; the background level can thus be seen to follow the data in the appropriate figures. The advantage of this procedure (as opposed to just cutting on the track isolation variable) for the low statistics on the tails of the distribution is that one can get some sense of the level of background from rare fragmentations of jets that may be topology dependent.
- [22] Decays before or after the COT volume result in a correct measurement of the momentum and are included in the other background estimate.
- [23] D. Acosta *et al.* (CDF Collaboration), Phys. Rev. D **71**, 032001 (2005).